J. Comp. App. Res. in Mech. Eng. Vol. 12. No. 1, pp. 77-93, 2022 *DOI: 10.22061/JCARME.2021.7514.1999*

Journal of Computational and Applied Research in Mechanical Engineering
jcarme.sru.ac.ir
SRTTU
JCARME
ISSN: 2228-7922

Research paper

Performance analysis of a combined cooling, heating and power system based on micro gas turbine from the point of view of exergy

J. Pirkandi[a,*], A. Amiralaei[b] and M. Ommian[a]

[a] *Faculty of Aerospace, Malek Ashtar University of Technology, Iran, 15875-1774*
[b] *Department of Mechanical Engineering, Azad University, West Tehran Branch, Iran, 1468763785*

Article info:

Article history:

Received: 15/11/2020
Revised: 09/12/2021
Accepted: 12/12/2021
Online: 14/12/2021

Keywords:
CCHP system,
Microturbine,
Absorption chiller,
Thermodynamic.

[*]Corresponding author:
Jamasb_p@yahoo.com

Abstract

In this research, a combined cooling, heating and power system (CCHP) has been analyzed from the perspective of entropy and exergy. The primary driver and the cooling system for this combined system consist of a micro gas turbine and a hot water lithium bromide single-effect absorption chiller, respectively. The effects of compressor pressure ratio, micro turbine inlet gas temperature and chiller cooling capacity on important system efficiencies and other operational parameters (e.g., electrical efficiency, thermal efficiency, combined heating and power cogeneration efficiency, and combined cooling, heating and power cogeneration efficiency) have been investigated. The findings indicate that the system has its highest electrical efficiency at a compressor pressure ratio of 5. Also at this pressure ratio, the cogeneration efficiency (combined heating, cooling and power) and the exergy efficiency are about 48% and 24%, respectively. Moreover, the increase of the turbine inlet gas temperature has had a positive effect on the investigated parameters. The results show that the increase of cooling capacity reduces the cogeneration efficiencies, but has no effect on the exergy efficiency. Also, by considering specific values for the studied parameters, the amounts of generated entropy and destroyed exergy in various parts of the system have been calculated. The results indicate that the highest amounts of entropy and exergy have been generated and destroyed in the combustion chamber. Parts of the results indicate a system state in which the overall efficiency (combined heating, cooling and power cogeneration efficiency) of the system has increased 13% relative to the system's initial state.

1. Introduction

In the last several decades, the growing worries and concerns about energy and fuel shortages have prompted research to find appropriate solutions and reformative measures aimed at reducing the level of fuel consumption and achieving higher efficiencies. One of the proposed mechanisms in this regard is the use of combined cooling, heating and power (CCHP) cogeneration systems [1]. Energy management will not be solely accomplished by striking a

balance between energy supply and demand, and it is necessary for the governments and policymakers to use appropriate strategies to achieve it [2]. One of the strategies that has greatly helped the technologically-advanced countries in the field of energy is the use of combined heating and power systems at the points of consumption [3]. These systems enable the cogeneration of power and heating in a single process. If such a process also includes cooling, it is called a cooling, heating and power cogeneration process. In general, CCHP systems consist of a primary driver (responsible for the generation of electricity), heat exchanger (for providing the needed heating) and chiller (for providing the cooling) [4]. Primary drivers come in various forms, including turbines, microturbines, fuel cells and reciprocating engines. For producing the cooling in these systems, equipment that can utilize the output wasted heat of a primary driver should be employed. Absorption chillers are the type of chillers that can utilize the energy of heat sources and, so, they can be used in cogeneration systems [5].

In recent years, numerous researchers have investigated the performance of cogeneration systems from various perspectives. Hwang [6] carried out a study on analyzing the performance of a cumulative cooling system along with microturbine and absorption chiller. In his proposed system, the wasted heat of the turbine was used to drive the absorption chiller, and the cooling produced by the chiller could be used to precool the air entering the microturbine or to cool a specific environment. Bruno et al. [7] have studied the performance of a microturbine connected with a double-effect hot water-lithium bromide absorption chiller. In their paper, they have analyzed the effect of gas afterburning, in two cases, on the performance of the hybrid system, at four different microturbine powers. Khaliq [8] presented a triple system based on a cycle of gas turbine, steam generation for heat recovery and an absorption chiller system. The proposed system was analyzed in terms of the first and second laws of thermodynamics. Ameri et al. [9] examined a cogeneration system from the standpoints of exergy and energy. In this research, they obtained the exergy destruction rate at all the cycle points as well as the exergy efficiency of every component of this system. Schicktanz et al. [10] examined the energy consumption and the feasibility of a combined heating, cooling and electricity cogeneration system. They focused on a practical small-scale system capable of producing 100 kW heating, 70 kW cooling and 58 kW electricity. Huicochea et al. [11] theoretically analyzed the thermodynamic performance of a triplet cogeneration system consisting of a microturbine and a double-effect hot water-lithium bromide absorption chiller. This research considered the conservation of mass and energy in all the major components of the cooling system based on the thermodynamic properties of water and lithium bromide as the working fluid. This triplet cogeneration system was analyzed under different conditions, including varying ambient temperature, generator temperature and microturbine fuel consumption rate. Ghaebi et al. [12] examined and optimized a triplet cogeneration system from exergy and economic perspectives. In their investigation, they employed the TRR method to economically model the system, and they used an evolutionary genetic algorithm for optimization. Jannelli et al. [13] studied a small-scale cogeneration system based on an internal combustion engine and a double-effect water-lithium bromide absorption chiller. In this system, the discharged thermal energy from the recuperator was used to produce hot water (for the heating system) and cold water (for the cooling system). Chen et al. [14] designed and analyzed the performance of a combined cooling, heating and power (CCHP) cogeneration system. This system included a small-scale gas turbine and a double-effect absorption chiller. In this research, they explored their introduced system from exergy and energy perspectives, and under partial load condition. Hanafizadeh et al [15] applied CCHP system for a commercial and office buildings in Tehran. In this regard, three different possible scenarios based on prime mover capacity are introduced and an economical study on each scenario is conducted to determine the optimal prime mover capacity for this building with regard to the availability of each alternative. Pirkandi et al. [16] presented thermoeconomic performance of a gas turbine based CHP cycle. Three design parameters of this cycle considered are compressor pressure ratio, turbine inlet temperature, and air mass flow rate.

Mohammadi et al. [17] proposed a hybrid system composed of a gas turbine, an ORC (Organic Rankine Cycle) cycle and an absorption refrigeration cycle as a combined cooling, heating and power system for residential usage. Huailiang You et al. [18] proposed a combined cooling, heating and power (CCHP), and multi-effect desalination system to supply cooling, heating, power and freshwater. Recently, a number of researchers such as Lingmin et al. [19] established modeling framework of a multi-energy system with coordinated supply of combined cooling, heating and power using wind and solar energy. Soltani et al. [20] compared a combined cooling, heating and power system with gas engine for energy demand of a commercial cold storage. Sheykhi et al. [21] proposed a combined cooling, heating and power system with a gas internal combustion engine prime mover. Asgari et al. [22] proposed an innovative trigeneration system including a gas turbine cycle, a gasification unit, a heating unit, alongside a single effect absorption refrigeration cycle. Yang et al. [23] presented a novel combined cooling, heating, and power system with a supercritical CO_2 Brayton cycle as the primary mover, wherein a part of heat that was originally released in the low temperature recuperator and a part of heat that was originally released to the environment are recovered for heating or cooling. These papers conducted research on the CCHP system with different approaches to study its effective use with the help of hybrid systems from the perspective of energy, exergy and economics. Peiravi et al. [24-27] have performed analytical studies and numerical solutions in this field.

A review of the conducted research shows that they all have considered an ideal system, without any pressure drop. Also, the performed analyses indicate that the examined systems have been evaluated more from an energy perspective and less from an exergy standpoint. Another point is the lack of an accurate and thorough investigation of the absorption chiller cycle in the majority of former works. In the present research, it has been attempted to consider the system's working conditions more realistically and to simulate all its losses. Moreover, the absorption chiller cycle has been modeled more completely and precisely. The operating conditions for the absorption chiller have been considered so as to have the chiller operating at its highest efficiency. Other achievements of this research are the investigation of the rate of exergy destruction and loss in the system and the determination of exergy efficiency for all cycle components.

In this research, a cogeneration system based on gas microturbine and single-effect absorption chiller from the perspective of exergy and the second law of thermodynamics has been analyzed. Most research in this field has focused on the second law of thermodynamics and the subject of exergy has received less attention. Determining the rate of degraded and wasted exergy in the components of the cycle and the whole system, determining the rate of entropy production, and determining the inefficient components are some of the important goals achieved in this research. On the other hand, the efficiency of the second law of the cycle and the efficiency of the CHP and CCHP systems have also been calculated and presented in this study. The main reason for determining the efficiency of CHP and CCHP is that in hot seasons of the year, the cooling and heating system (to provide sanitary hot water) is used simultaneously, and in cold seasons, only the heating system (for heating and sanitary hot water) is used.

2. System description

The proposed system includes a micro gas turbine for generating electricity and a hot water-lithium bromide absorption chiller for providing the needed cooling (Fig. 1). The fuel utilized in this system is natural gas (methane), which is compressed and preheated by passing through the compressor and the heat exchanger. Similarly, air is compressed and preheated by passing through the compressor and the heat exchanger and then it is mixed with the incoming fuel and burned in the combustion chamber. The hot combustion gases, after passing through the turbine and generating electricity, first enter the two mentioned heat exchangers in order to preheat the incoming air and fuel, and then enter the third and fourth heat exchangers to produce hot water. The third heat exchanger provides warm or hot water for the absorption chiller, and the fourth heat exchanger provides warm water for washing and sanitary purposes as well as other heating requirements.

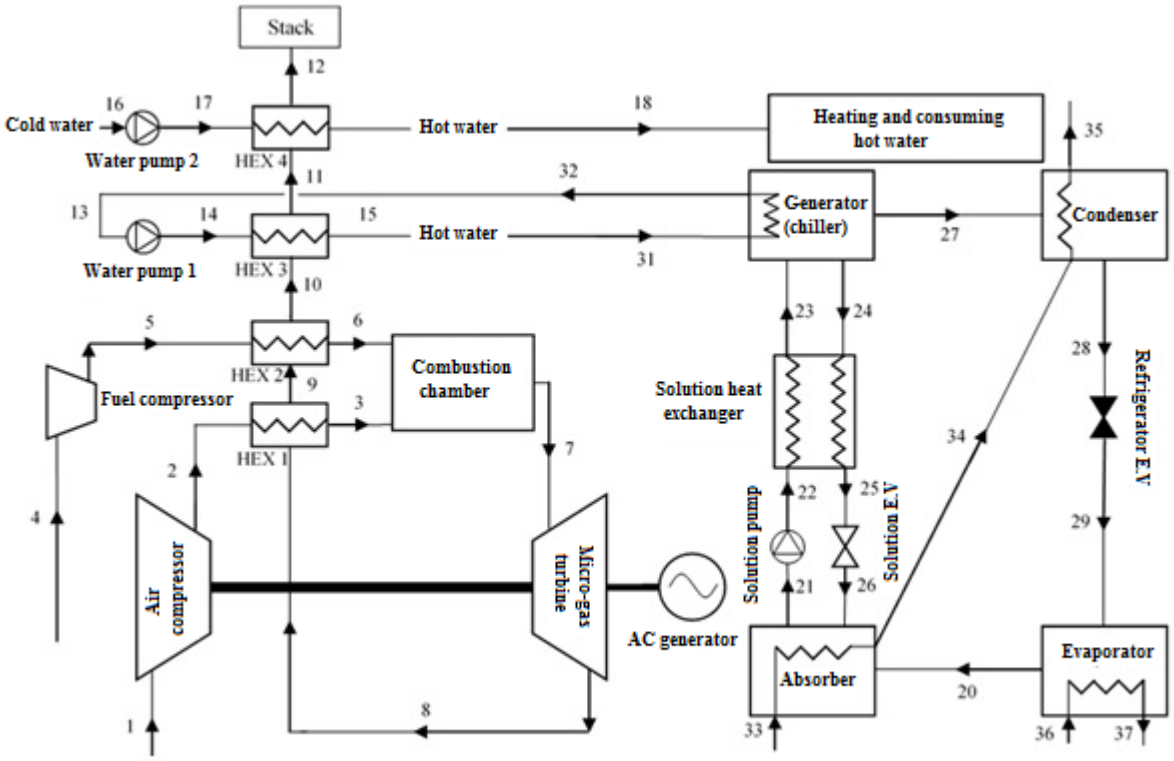

Fig. 1. Diagram of proposed system cycle.

The present paper is a theoretical work and its results can be used in a real system. In recent years, research on CCHP systems has grown significantly and the use of this system in practical buildings, commercial, office, medical, residential towers, etc. has grown more and more. Studies show that the return on investment of this type of system is under 5 years and their use can help reduce electricity consumption in the summer. On the other hand, these systems are independent and can be generated by selling electricity to the electricity network. The use of this system is recommended for buildings with high electricity consumption and cost. Another important point is the low gas consumption and cost of buildings with CCHP systems, which will also reduce the current cost of this system.

3. Assumptions

In this research, the following assumptions have been considered in solving the problem:

- The analysis has been performed for a steady flow condition.
- The cooling fluid (water) at condenser outlet is saturated liquid.
- The cooling fluid (water) at evaporator outlet is saturated vapor.
- The lithium bromide solution at the absorber outlet is a dilute solution at absorber temperature.
- The temperature of the cooling fluid and the solution exiting a generator is the same as the generator temperature.
- Pressure drop along the tubes has been ignored.
- A 7% pressure drop has been considered along the tube line from the outlet of chiller generator to pump inlet.
- The cold water that enters the system from the cooling tower goes right into the condenser, after passing through the absorber.
- The exchange of heat between system and environment and between environment and chiller components (generator, condenser, absorber and evaporator) has been disregarded.

- Gas leakage from within the system to the outside has been ignored.
- Fluid flow in the compressor and turbine has been considered as adiabatic.
- The variations of kinetic and potential energies and the exergies associated with them have been ignored.
- All the existing gases in the cycle have been assumed to behave as ideal gases.
- The reference values for the environment (basic state) are as follows: ambient temperature = 25 ºC, pressure = 1 atm., and concentration = 50%.

The other inputs and parameters assumed for the system have been listed in Table 1 and Table 2.

Table 1. System input values.

Parameter	Value
Evaporator temperature (°C)	4~10
Condenser temperature (°C)	33~39
Absorber temperature (°C)	33~39
Generator temperature (°C)	60~135
Inlet water temperature to condenser (°C)	-8
Water outlet temperature of the condenser (°C)	-3
Inlet water temperature to evaporator (°C)	+8
Water outlet temperature of the evaporator (°C)	+3
Inlet water temperature to generator (°C)	+18
Water outlet temperature of the generator (°C)	+8
Inlet water temperature to absorber (°C)	-8
Water outlet temperature of the absorber (°C)	-3
Ambient temperature (°C)	25
Ambient pressure (kPa)	101
Pump efficiency	0.95
Effectiveness	0.7
Water specific value (kJ/kg.K)	4.18
Heat transferred to the evaporator (kW)	300

4. Governing equations

Some of the governing equations of the analyzed system are as follows [1]:

Chiller:

The law of the conservation of concentration can be written as:

$$\Sigma m_i x_i = \Sigma m_o x_o \quad (1)$$

where X is the concentration of lithium bromide in the solution.
Concentration is defined as:

$$X = \frac{m_l}{m_l + m_w} \quad (2)$$

where indexes l and w are used for lithium bromide and water, respectively.
The chiller performance coefficient is defined as follows:

$$COP = \frac{Q_{eva}}{Q_{gen} + W_P} \quad (3)$$

In the above equation, COP denotes the coefficient of performance, Q_{eva} is the energy absorbed from the evaporator and Q_{gen} is the energy input into the chiller generator.
Exergy analysis combines the first and the second laws of thermodynamics. Exergy is defined as the greatest amount of work that can be done by a flow or a system when going from its existing state to a state in equilibrium with the environment [28]. The overall change of real exergy between the inputs and outputs of a control volume is equal to the sum of reversibility and irreversibility fractions. This overall change is called the real exergy. In this equation, due to the lack of heat transfer, the relevant term has been omitted.
The exergy efficiency [2] is obtained from Eq. (4).

$$\eta_{exergy} = \frac{Q_{eva} \cdot \left(1 - \frac{T0}{Tb}\right)}{\left[Q_{gen} \cdot \left(1 - \frac{T0}{Th}\right) + Wp\right]} \quad (4)$$

In the above equation, W_p is the mechanical work of pump, T_b is the average temperature of the cold source (in the evaporator) and T_h is the

average temperature of the hot source (in the generator).

Compressor:

Compressor work is obtained from thermodynamic relationships [1].

$$\dot{W}_{ac}=\dot{n}_a(h_2-h_1) \quad (5)$$

In the above equations, n_a is the flow rate of air entering the compressor. Also, W_{ac} is the real work required by compressor. Considering the dependency of isentropic efficiency on pressure ratio and its fluctuations with pressure changes, in case pressure ratio variations are considered in system analysis, polytropic efficiency (η_p) is used instead of isentropic efficiency.

$$\eta_{is,ac}=\frac{(r_{p,a})^{\frac{k_a-1}{k_a}}-1}{(r_{p,a})^{\frac{k_a-1}{k_a.\eta_{p,ac}}}-1} \quad (6)$$

Fuel compressor calculations are similar to those of air compressor.

Combustion chamber:

As is observed in Fig. 1, the compressor's outlet air is warmed by a heat recuperator before entering the combustion chamber. In this chamber, air reacts with the incoming fuel, which has itself been warmed by another heat exchanger. In these ranges of temperature and pressure, without introducing a serious error into the computations, air and the combustion products are considered as ideal gases. By assuming complete combustion for fuel and writing the energy conservation equation and by considering the efficiency of the chamber, the temperature of outlet gases can be determined [1].

$$n_3 h_3+n_6 h_6-n_7 h_7-Q_{Loss,cc}=0 \quad (7)$$

This relation is related to the first law of thermodynamics in the combustion chamber.

$$Q_{Loss,cc}=\dot{n}_f\times(1-\eta_{cc})\times\mathrm{LHV} \quad (8)$$

In the above equation, $Q_{Loss,cc}$ denotes the heat losses of the combustion chamber and its value depends on fuel flow rate, combustion chamber efficiency, and the heating value of fuel.

Microturbine

By computing the ideal work of the turbine and considering its isentropic efficiency, the output work and the temperature of the turbine can be calculated by the following equations [29]:

$$\dot{W}_{mgt}=\dot{n}_7(h_8-h_7) \quad (9)$$

In the above equations, n is the flow rate of fuel entering the turbine.

As was mentioned earlier, considering the dependency of isentropic efficiency on pressure ratio, and in case compressor pressure ratio variations are considered in system analysis, polytropic efficiency (η_p) is used instead of isentropic efficiency.

$$\eta_{is,mgt}=\frac{1-\left(\frac{1}{r_{p,mgt}}\right)^{\frac{\eta_{p,mgt}(k_g-1)}{k_g}}}{1-\left(\frac{1}{r_{p,mgt}}\right)^{\frac{k_g-1}{k_g}}} \quad (10)$$

Recuperators:

For raising the temperature of the air and the fuel entering the combustion chamber and also for providing the needed hot water, two external recuperators, fed by the microturbine's hot exhaust gases, have been used [30]. For example, by considering the effectiveness of the third recuperator, the following equations are used to determine the useful thermal load in this recuperator:

$$Q_{HEX3}=\varepsilon_{HEX3}\dot{n}_{11}(h_{11}-h_{10}) \quad (11)$$

$$Q_{HEX3}=\dot{n}_{water1}.\bar{c}_p.(T_{15}-T_{14}) \quad (12)$$

Hybrid system:

In this section, by considering the whole system as a control volume, system efficiencies will be obtained through the following equations [31]:

$$\eta_{elec}=\frac{\dot{W}_{net}}{\dot{n}_f\times LHV} \quad (13)$$

$$\eta_{th}=\frac{Q_{HEX4}}{\dot{n}_f\times LHV} \quad (14)$$

$$\eta_{CHP}=\frac{\dot{W}_{net}+Q_{HEX4}}{\dot{n}_f\times LHV} \quad (15)$$

$$\eta_{CCHP}=\frac{\dot{W}_{net}+Q_{HEX4}+Q_{eva}}{\dot{n}_f\times LHV} \quad (16)$$

$$\eta_{exergy,tot}=\frac{\dot{W}_{net}+Q_{eva}\cdot\left(1-\frac{T_0}{T_b}\right)+\dot{E}_{18}}{\dot{E}_1+\dot{E}_4+\dot{E}_{16}} \quad (17)$$

In the above equations, $\dot{n}_f$ denotes the flow rate of fuel entering the fuel compressor. The system's net output power is the same as microturbine's, and the amount of the energy entering the system is equal to the energy released by burning the fuel in the combustion chamber [31]. Also, η_{elec} is the electrical efficiency, η_{th} the thermal efficiency, η_{CHP} the combined heating and power efficiency, η_{CCHP} the combined cooling, heating and power efficiency, and $\eta_{exergy,tot}$ is the total exergy efficiency of the system.

$$\dot{W}_{net}=\left(\dot{W}_{AC\text{-}net}\right)_{mgt} \quad (18)$$

$$\left(\dot{W}_{AC\text{-}net}\right)_{mgt}=(\dot{W}_{DC})_{mgt}\times\eta_{inv,gen}-\dot{W}_{wp1}-\dot{W}_{wp2}-\dot{W}_p-\dot{W}_{ac}-\dot{W}_{FC} \quad (19)$$

$$(\dot{W}_{DC})_{mgt}=\dot{W}_{mgt} \quad (20)$$

In Eq. (19), $\eta_{inv.gen}$ represents the direct current-to-alternating current conversion coefficient for microturbine generator [32].

5. Solution algorithm

To analyze the proposed system, the microturbine and the series flow single-effect absorption chiller have been separately modeled in the Engineering Equation Solver (EES) software, based on the equations given in the Governing Equations section. Then the two written codes have been coupled together and used as a single program. EES is a software program for solving engineering equations; and thermodynamic equations are given to the program using the thermodynamic specifications of various points (temperature, pressure, enthalpy, etc.), which are available in the software itself. In the next step, the software program considers these equations as a system of equations and, using an initial guess, starts to solve them by means of common numerical techniques. The overall solution approach is the iteration method, which repeats the computations until the residual value determined by the user for each parameter is reached.

6. Results and discussion

6.1. Validation

In this section, the paper of Gomri [33] has been used to validate the code written for the chiller. This paper includes two sections on a single-effect absorption chiller and a series flow double-effect absorption chiller. For validation purposes, the chiller here has been modeled by using the inputs considered in Gomri's research, and the results of this model have been compared with those of Gomri's. The inputs used have been listed in Table 1. It should be mentioned that in this section, the same working temperature has been considered for the absorber and the condenser. The results obtained for the analyzed single-effect absorption chiller have been presented in Table 2. This table contains the performance coefficients of the absorption chiller at several generator temperatures, four different evaporator temperatures and various condenser temperatures. These values include the results of Gomri's work and the results obtained from the modeling used in this research. The differences between these results have also been given in a separate column. By examining the presented results and the differences between Gamri's results and those of this research, the accuracy of the modeling in this work can be affirmed.

In order to validate the code prepared for microturbine, it is necessary to compare the results of this code for a specific sample with the results of the existing research. In this research, the system introduced by Horlock [34] has been modeled and its results have been compared with those obtained from the present code. The close agreement between these results in Table 3 confirms the validity of the present approach and the prepared code.

6.2. Effect of compressor pressure ratio

In this section, the effect of compressor pressure ratio on the parameters and efficiencies of the proposed system has been investigated. These parameters and efficiencies include the system's net output power, transferred heat for heating

purposes, electrical efficiency, combined heating and power efficiency, combined cooling, heating and power efficiency, and the exergy efficiency.

The molar flow rate of air entering the compressor is 400 kmole/hr, the temperature of stack gases (T_{stack}) is 200 ºC and the cooling capacity of chiller is 205 kW. The variation of the compressor pressure ratio has been analyzed at three different turbine inlet temperatures (TIT). The constant parameters assumed in this section have been presented in Table **4**. As is observed in Fig. **3**, the total output electrical power initially goes up with the increase of the compressor pressure ratio and reaches a maximum value, and then, with the further increase of compressor pressure ratio, it starts to decline and almost reaches its initial value. The reason for this is the extra work by compressors to raise the pressure, and thus the reduction of the system's net output power.

The system achieves its maximum total output electrical power at a compressor ratio of 4 to 6. It is also observed that by raising the turbine inlet temperature, the system's power output increases. However, due to the temperature tolerance limitation of microturbine rotors, the temperature cannot be raised higher than 1000 ºC. Fig. 4 shows that the electrical efficiency has a trend which is similar to the system's output electrical power; and that it achieves its maximum value at a specific range of compressor pressure ratio. The diagrams of thermal load and thermal efficiency versus compressor pressure ratio have been illustrated in Fig. 5 and Fig. 6, respectively. According to these figures, thermal load (for heating purposes) and thermal efficiency increase considerably with the increase of compressor pressure ratio. The rise in turbine inlet temperature also increases the thermal load and thermal efficiency. The cause of this increase could be the increase in the temperature of Point 11 with the increase of compressor pressure ratio. An important point to consider is that by increasing the compressor pressure ratio, the thermal efficiency approaches the same value at three different turbine inlet temperatures.

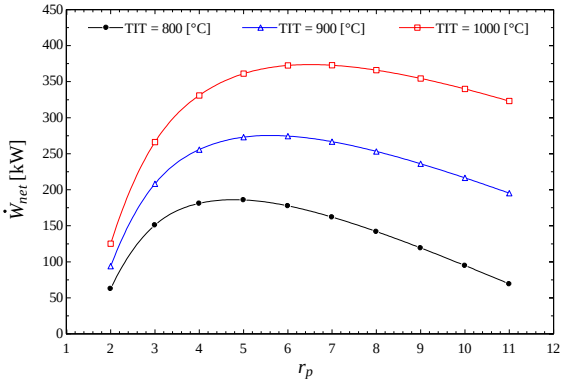

Fig. 2. Total electrical power output as function of compressor pressure ratio.

Table 2. Comparison of coefficient of performance of hot water single effect absorption chiller in Tcond=33 ºC.

Generator temperature	Gomri results [33]	Present work	Error (%)
	T_{eva} = 4 ºC		
75	0.74	0.7604	2.7
85	0.76	0.7785	2.4
95	0.76	0.7786	2.4
105	0.75	0.7777	3.7
	T_{eva} = 6 ºC		
75	0.75	0.784	4.5
85	0.77	0.791	2.7
95	0.77	0.787	2.2
105	0.76	0.785	3.2
	T_{eva} = 8 ºC		
75	0.77	0.802	4.1
85	0.775	0.801	3.3
95	0.775	0.796	2.7
105	0.77	0.792	2.8
	T_{eva} = 10 ºC		
75	0.78	0.817	4.7
85	0.79	0.812	2.7
95	0.78	0.805	3.2
105	0.775	0.799	3.1

Table 3. Comparison between current study and horlock's results**.**

	Present work	Horlock results [34]	Error (%)
Efficiency (%)	35.8	34.5	3.77
Power consumed by compressor (kW)	358	350	2.3
The power generated by the turbine (kW)	672	650	3.4
Generated net power (kW)	312	300	4

Table 4. Assumed parameters in proposed system

Parameter	Assumed value (%)
Recuperate pressure drop	4
Combustion chamber pressure drop	5
Compressor isentropic efficiency	81
Air-gas recuperator effectiveness	80
Water-gas recuperator effectiveness	85
Water pump efficiency	95
Combustion chamber efficiency	95
Microturbine isentropic efficiency	84
Generator efficiency	95
Chiller pressure drop	3

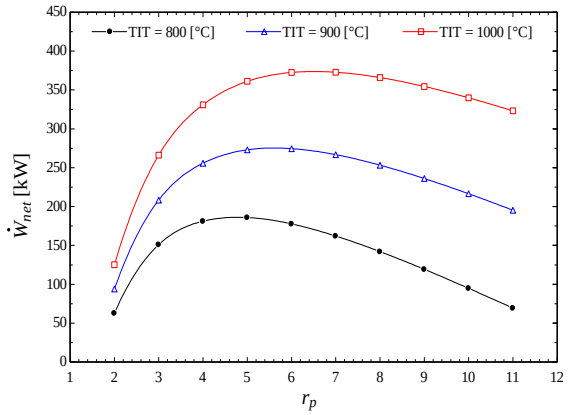

Fig. 3. Total electrical power output as function of compressor pressure ratio.

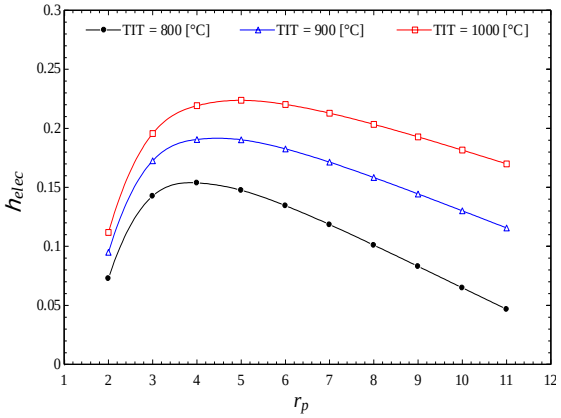

Fig. 4. Electrical efficiency as function of compressor pressure ratio.

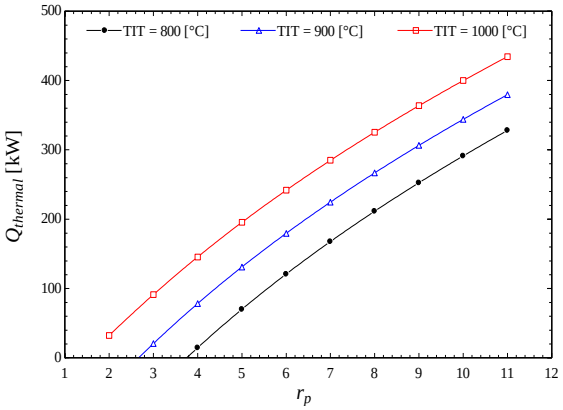

Fig. 5. Heating load as function of compressor pressure ratio.

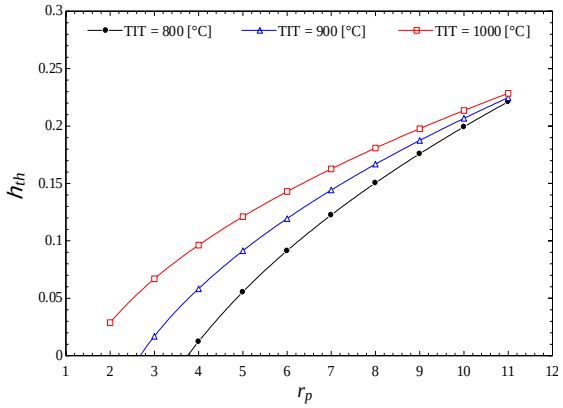

Fig. 6. Thermal efficiency as function of compressor pressure ratio.

Fig. 7 and Fig. 8 show the efficiencies of the CHP and CCHP systems versus compressor pressure ratio. As is observed, by raising the pressure ratio, these efficiencies are increased, first with a sharp slope, and then with a milder slope. The reason for this increase is the increase in the system's thermal load and output electrical power. Fig. 9 illustrates the system's total exergy efficiency versus compressor pressure ratio. Exergy efficiency also increases up to a maximum value (about 5) initially, and then diminishes. Exergy efficiency behaves, which shows a similar behavior for exergy efficiency and output electrical power. With respect to the impact of compressor pressure ratio on various system parameters, it can be concluded that a pressure ratio of 5 will be the optimal compressor pressure ratio at which the examined parameters could achieve their maximum values.

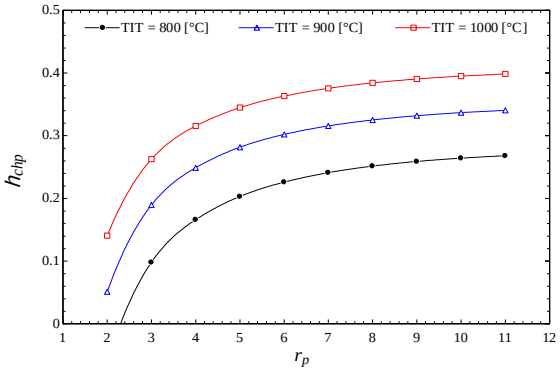

Fig. 7. Combined heating and power efficiency as function of compressor pressure ratio

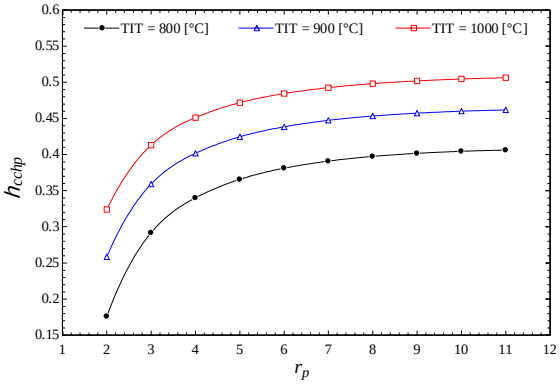

Fig. 8. Combined heating, cooling and power efficiency as function of compressor pressure ratio

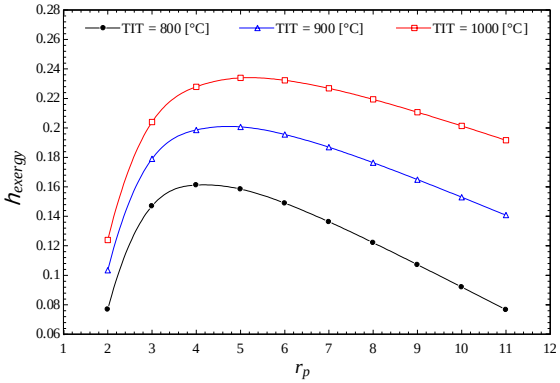

Fig. 9. Total exergy Efficiency of the System as function of compressor pressure ratio

Fig. 10, Fig. 11 and Fig. 12 respectively show the system's total entropy generation rate, total exergy destruction rate and total exergy loss rate of the system. As is observed, these parameters increase with the rise of compressor pressure ratio. The underlying cause is the increase in the amount of energy which is present in the cycle, and consequently the high rates for these parameters.

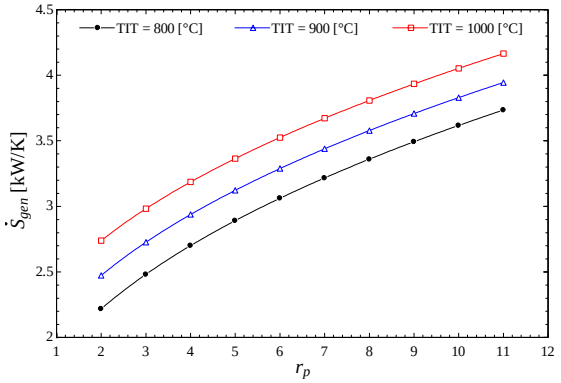

Fig. 10. Generated entropy rate of the system as function of compressor pressure ratio.

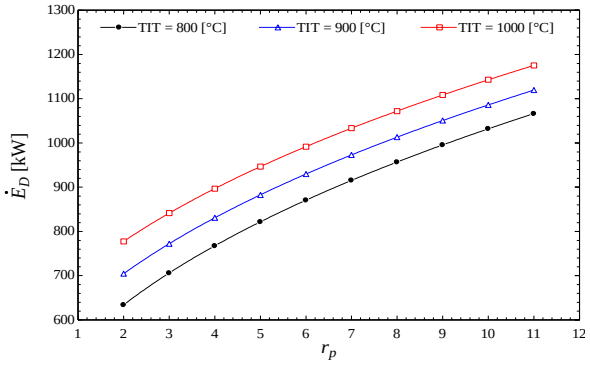

Fig. 11. Destroyed exergy rate of the system as function of compressor pressure ratio.

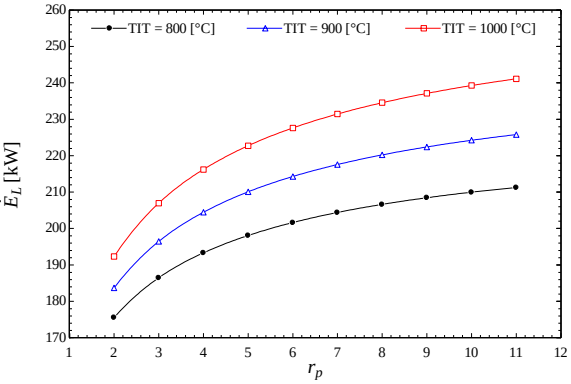

Fig. 12. Lost exergy rate of the system as function of compressor pressure ratio.

6.3. Effect of the cooling capacity of absorption chiller

Several diagrams related to the effects of system parameters at three different chiller loads have been presented in the following section. In these graphs, the molar flow rate of the air entering the compressor and the turbine inlet temperature have been considered as 1000 kmole/hr and 1000

ºC, respectively. Fig. 13 and Fig. 14 indicate that by increasing the chiller's cooling power, the thermal load for heating applications and also the CHP efficiency are reduced. The reason for this reduction is that, in order to supply more cooling, the chiller receives a greater amount of energy from the energy-carrying gases and therefore, less energy is left for the next cycle, which is the cycle for heating applications. The variations of CCHP efficiency and exergy efficiency have been illustrated in Fig. 15 and Fig. 16, respectively. Similar to CHP efficiency, CCHP efficiency diminishes with the increase of chiller's cooling load; but this reduction is negligible relative to that of CHP efficiency; because despite the reduction of the heating load, the system's cooling load increases and compensates for the heating load deficiency. So it can be concluded that CCHP efficiency does not change significantly with the changes of chiller's cooling load. Fig. 16 shows that the total exergy efficiency of the system is not affected by the chiller's cooling load.

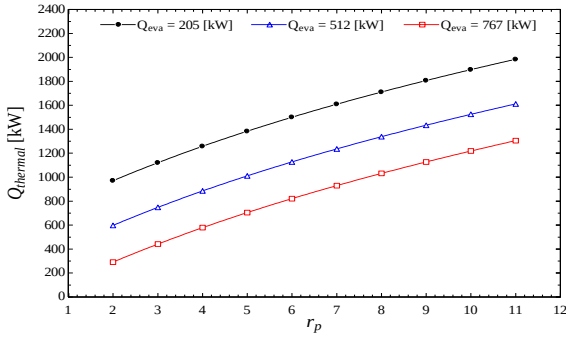

Fig. 13. Heating load as function of compressor pressure ratio and three different cooling capacity of absorption chiller.

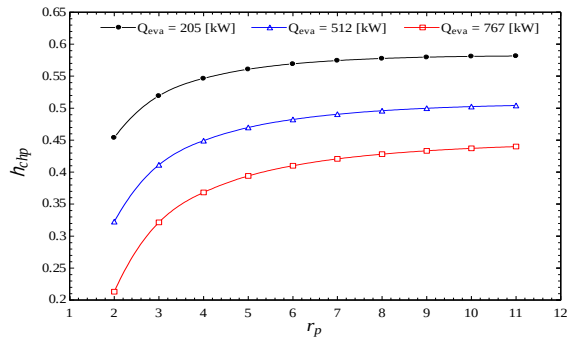

Fig. 14. Combined heating and power efficiency as function of compressor pressure ratio and three different cooling capacity of absorption chiller.

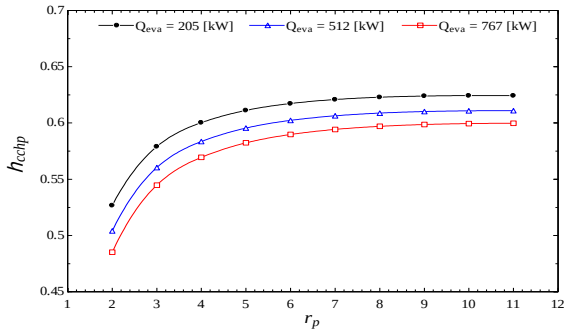

Fig. 15. Combined cooling, heating and power efficiency as function of compressor pressure ratio and three different cooling capacity of absorption chiller.

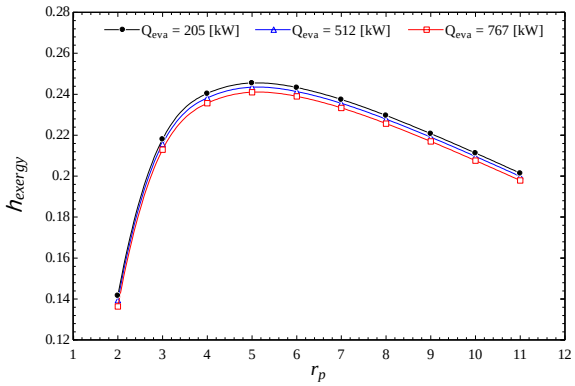

Fig. 16. Total exergy efficiency of the system as function of compressor pressure ratio and three different cooling capacity of absorption chiller

6.4. Entropy and exergy analyses

Fig. 17 and Fig. 18 respectively show the entropy generation rate and exergy destruction rate in various components of the CCHP system, except those of the absorption chiller, at a specific system state which has been considered for comparison purposes.

The input and output values, which is the most optimal state of the system, have been presented in Table 5 It should be mentioned that the temperature of the turbine inlet gases is 1000 ºC. According to Fig. 17 and Fig. 18, the highest amount of entropy generation and exergy destruction occurs in the combustion chamber; because in this chamber, a part of the thermal energy produced through combustion is transferred to the surrounding environment and wasted.

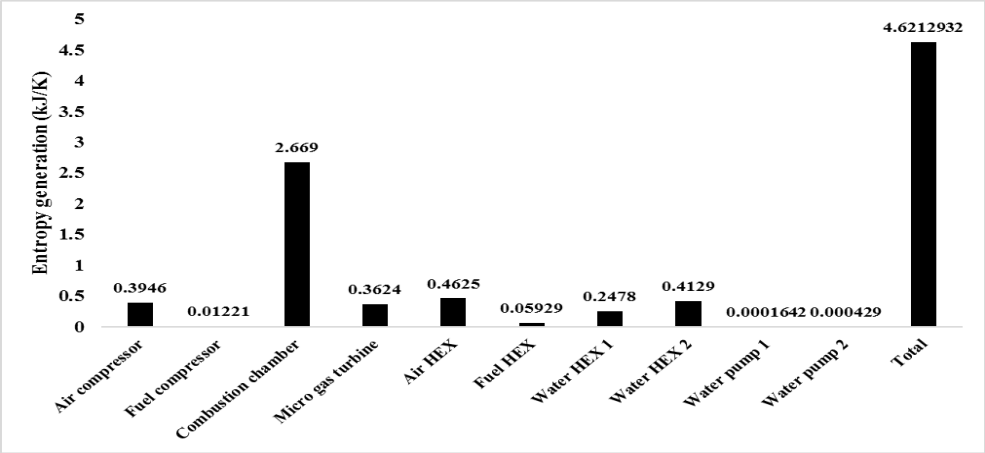

Fig. 17. Chart of generated entropy in CHP parts

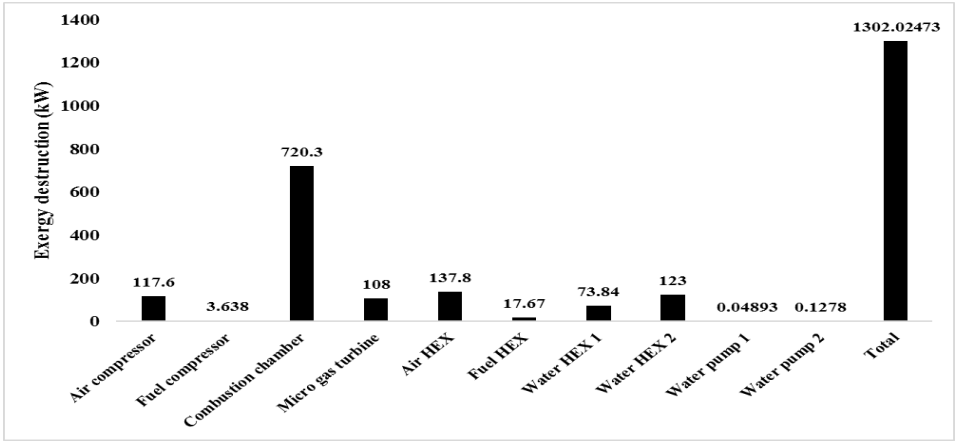

Fig. 18. Chart of destroyed exergy in CHP parts.

Fig. 19 and Fig. 20 show the entropy generation rate and exergy destruction rate in various components of the hot water-lithium bromide single-effect absorption chiller. It is observed that the highest values of these parameters occur in the generator, followed by the absorber. The reason for this is the greater amount of heat exchange in the generator and absorber compared to other components.

Table 5. Parameters and efficiencies of the cycle in optimum operating state.

Parameter	Value
Inlet air flow rate	553 kmol/h
Outlet gas temperature	127 °C
Inlet air temperature	25 °C
Cooling load	205 kW
Compressor pressure ratio	5
Outlet electrical power	500 kW
Electrical efficiency	22.33 %
Thermal efficiency	29.24 %
CHP efficiency	51.58 %
CCHP efficiency	60.74 %
Exergy efficiency	24.65 %
Generator heating load	247 kW
Condenser heating load	214.6 kW
Absorber heating load	239 kW
Chiller coefficient of performance	0.81

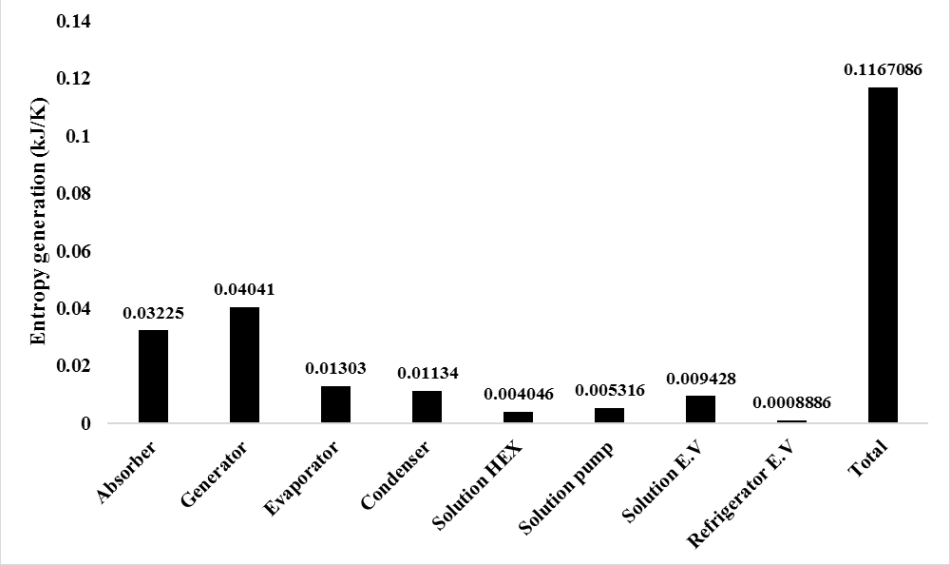

Fig. 19. Chart of generated entropy in the absorption chiller

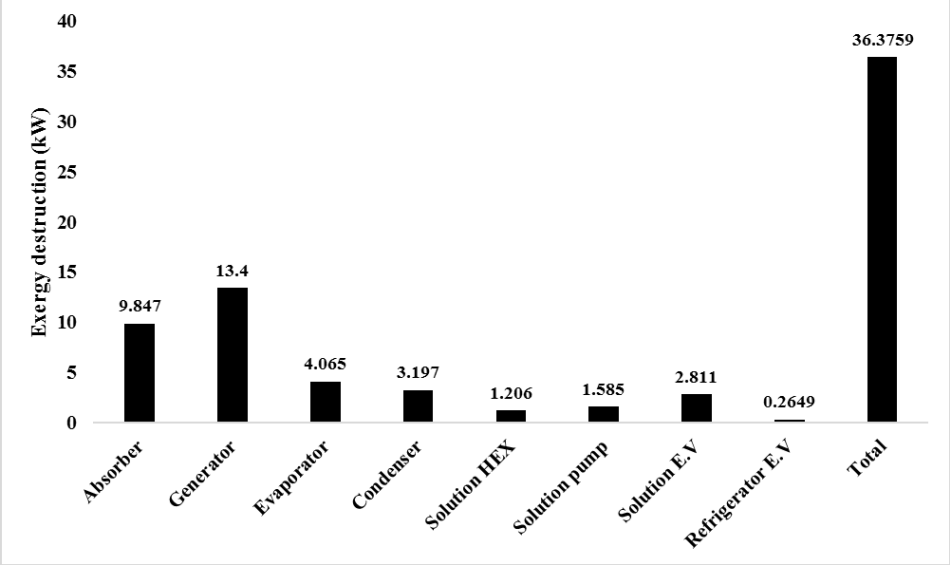

Fig. 20. Chart of destroyed exergy in the absorption chiller

7. Conclusions

The findings of this research are as follows:
A rise in the turbine inlet temperature, because of increasing the energy input of the microturbine, increases the output electrical power, electrical efficiency, thermal efficiency, CHP and CCHP efficiencies, exergy efficiency, total entropy generation rate, total exergy destruction rate, and the exergy loss rate of the proposed system.

Increasing the compressor pressure ratio up to a certain point increases the output electrical power of the considered system and its electrical efficiency; however, a further increase of pressure ratio beyond that point reduces the system's electrical power and efficiency. The reason for this is the increase in the amount of energy utilized by the compressor, and thus the reduction in the net power output of the microturbine. This behavior is also true for exergy efficiency; however, with the increase of pressure ratio, the thermal, CHP and CCHP

efficiencies increase. In general, there is a range of compressor pressure ratio in which the system exhibits optimal performance. Also, by raising the compressor pressure ratio, an increase is observed in the proposed system's total entropy generation rate, total exergy destruction rate, and the exergy loss rate.

An increase in the cooling capacity of the lithium bromide single-effect absorption chiller has no effect on output electrical power and electrical efficiency; but by increasing the energy received by the chiller cycle and cutting down the energy received by the heating production cycle along the way, the thermal load and efficiency, CHP efficiency and CCHP efficiency reduce. The system's total entropy generation rate, total exergy destruction rate and the exergy loss rate do not change with the increase of cooling load, because the greater amount of energy received by the chiller only affects the chiller cycle.

The optimum operating state of the proposed system is achieved at an input air flow rate of 553 kmole/hr, turbine input temperature of 1000 ºC, compressor input temperature of 25 ºC, exhaust gas temperature of 127 ºC, and a cooling load of 205 kW. In this state, the overall system efficiency (i.e. CCHP efficiency) increases by about 13% relative to the initial state considered for the system (the abovementioned parameters in the initial state are 400 kmole/hr, 1000 ºC, 25 ºC and 200 ºC, respectively).

In the optimal state of the system, the greatest amount of the destroyed exergy and generated entropy belongs to the combustion chamber, and in the chiller, to the generator and the absorber units. The reason for this is the existence of high thermal energy in these components.

Results show that the gas microturbine cycle has a major contribution to the inefficiency of the entire CCHP system compared to the absorption chiller cycle. On the other hand, the results show that the combustion chamber of the gas microturbine cycle has the highest rate of exergy degradation and entropy production rate in the whole cycle. In the combustion chamber, by improving the combustion chamber design, reducing heat loss, improving fuel-air mixing, etc., the inefficiency of this component can be reduced. In the absorption chiller cycle, the most exergy destruction and loss is related to the absorption chiller generator. For any improvement in the performance of the absorption chiller cycle, the focus must be on these two components. Regarding the absorption chiller generator, due to the fact that this component is a heat exchanger, it is possible to create better conditions for better heat transfer and better concentration of lithium bromide by using finned and grooved pipes with suitable materials. Using two or three generators for concentration is another way to improve the chiller performance.

Key and critical points of this paper are:

The highest rate of exergy destruction in the CCHP cycle is related to the primary generator (gas microturbine cycle) and this cycle has a higher inefficiency compared to the absorption chiller.

In the primary generating components (gas microturbine cycle), the main part is related to the combustion chamber. The main reason for this is the chemical reactions and heat loss.

In the secondary generating components (absorption chiller cycle), the main inefficiency is related to the generator and chiller absorber. The reason for this is the concentration of lithium bromide in the generator and the absorption of water vapor in the absorber.

Parametric analysis in this study also shows that the excessive increase of the pressure ratio is not appropriate and increases the inefficiency of the cycle components. Parametric analysis shows that the appropriate pressure ratio for the proposed system is in the range of 4 to 6.

8. References

[1] M. Ebrahimi, and A. Keshavarz, "Combined cooling, heating and power", Elsevier Publisher, ISBN: 9780080999852, pp. 45-80, (2014).

[2] P. Gao, Y. Daib, Y. Tong and P. Dong, "Energy matching and optimization analysis of waste to energy CCHP (combined cooling, heating and power) system with exergy and energy level", *J. Energy*, Vol. 79, No. 1, pp. 522-535, (2015).

[3] H. Cho, A. D. Smith and P. Mago, "Combined cooling, heating and power: A review of performance improvement and optimization", *Appl. Energy*, Vol. 136, No.

1, pp. 168–185. (2014).
[4] P. Chen, L. Guan, Z. Tang, X. Chen and Z. Jiang, "An optimal planning method for combined cooling heating and power system", *Energy Procedia*, Vol. 103, No. 1, pp. 123 – 128, (2016).
[5] N. Fumo and L. M. Chamra, "Analysis of combined cooling, heating, and power systems based on source primary energy consumption", *Appl. Energy*, Vol. 87, No. 1, pp. 2023–2030. (2010).
[6] Y. Hwang, "Potential energy benefits of integrated refrigeration system with microturbine and absorption chiller", *Int. J. Refrig.*, Vol. 27, No. 8, pp. 816–829, (2004).
[7] J. C. Bruno, A. Valero and A. Coronas, "Performance analysis of combined microgas turbines and gas fired water/LiBr absorption chillers with post-combustion", *Appl. Therm. Eng.*, Vol. 25, No. 1, pp. 87–99, (2005).
[8] A. Khaliq, "Exergy analysis of gas turbine trigeneration system forcombined production of power heat and refrigeration", *Int. J. Refrig.*, Vol.32 , No. 1, pp. 534 – 545 , (2009).
[9] M. Ameri, A. Behbahaninia, and A. A. Tanha, " Thermodynamic analysis of a tri-generation system based on micro-gas turbine with a steam ejector refrigeration system", *J. Energy*, Vol. 35, No. 5, pp.2203-2209, (2010).
[10] M. D. Schicktanz, J. Wapler and H. M. Henning, "Primary energy and economic analysis of combined heating, cooling and power systems", *J. Energy*, Vol. 36, No. 1, pp.575-585, (2011).
[11] A. Huicochea, W. Rivera, G. Gutiérrez-Urueta, J. C. Bruno and A. Coronas, "Thermodynamic analysis of a trigeneration system consisting of a micro gas turbine and a double effect absorption chiller", *Appl. Therm. Eng.*, Vol. 31, No. 16, pp. 3347-3353, (2011).
[12] H. Ghaebi, M. H. Saidi and P. Ahmadi, "Exergoeconomic optimization of a trigeneration system for heating, cooling and power production purpose based on TRR method and using evolutionary algorithm", *Appl. Therm. Eng.*, Vol. 36, No. 1, pp.113-125, (2012).
[13] E. Jannelli, M. Minutillo, R. Cozzolino and G. Falcucci, "Thermodynamic performance assessment of a small size CCHP (combined cooling heating and power) system with numerical models", *J. Energy*, Vol. 65, No. 1, pp. 240-249, (2014).
[14] Q. Chen, W. Han, J. Zheng, J. Sui and H. Jin, "The exergy and energy level analysis of a combined cooling, heating and power system driven by a small scale gas turbine at off design condition", *Appl. Therm. Eng.*, Vol. 66, No. 1, pp 590-602, (2014).
[15] P. Hanafizadeh, J. Eshraghi, P. Ahmadi and A. Sattari, " Evaluation and sizing of a CCHP system for a commercial and office buildings" *J. Build. Eng.*, Vol. 5, No. 1, pp 67-78, (2016).
[16] J. Pirkandi, M. A. Jokar, M. Sameti, A. Kasaeian and F. Kasaeian, " Simulation and multi-objective optimization of a combined heat and power (CHP) system integrated with low-energy buildings" *J. Build. Eng.*, Vol. 5, No. 1, pp 13-23, (2016).
[17] A. Mohammadi, A. Kasaeian, F. Pourfayaz and M. H. Ahmadi, "Thermodynamic analysis of a combined gas turbine, ORC cycle and absorption refrigeration for a CCHP system", *Appl. Therm. Eng.*, Vol. 111, No. 1, pp. 397-406, (2017).
[18] H. You, J. Han and Y. Liu, "Performance assessment of a CCHP and multi-effect desalination system based on GT/ORC with inlet air precooling", *J. Energy*, Vol. 185 No. 1, pp. 286-298, (2019).
[19] C. Lingmin, W. Jiekang, W. Fan , T. Huiling , L. Changjie and X. Yan, "Energy flow optimization method for multi-energy system oriented to combined cooling, heating and power" *J. Energy*, Vol. 211, No. 1, 118536, (2020)
[20] M. Soltani, M. Chahartaghi, M. Hashemian and A. Faghih Shojaei, "Technical and economic evaluations of combined cooling, heating and power (CCHP) system with gas engine in commercial cold storages", *Energy Convers. Manage.*, Vol. 214, No. 1, 112877, (2020).
[21] M. Sheykhi, M. Chahartaghia, A.Safaei, P.

Richard and G.J.Flay, "Investigation of the effects of operating parameters of an internal combustion engine on the performance and fuel consumption of a CCHP system", *J. Energy*, Vol. 211, No. 1, 119041, (2020).

[22] N. Asgari, R. Khoshbakhti Saray and S. Mirmasoumi, "Energy and exergy analyses of a novel seasonal CCHP system driven by a gas turbine integrated with a biomass gasification unit and a LiBr-water absorption chiller", *Energy Convers. Manage.*, Vol. 220, No. 1, 113096, (2020).

[23] Y. Yang, Y. Huang, P. Jiang and Y. Zhu, "Multi-objective optimization of combined cooling, heating, and power systems with supercritical CO2 recompression Brayton cycle", *Appl. Energy*, Vol. 271, No. 1, 115189, (2020).

[24] M. M. Peiravi and J. Alinejad, "Nano particles distribution characteristics in multi-phase heat transfer between 3D cubical enclosures mounted obstacles", *Alexandria Eng. J.*, Vol. 60, No. 6, pp 5025-5038 (2021).

[25] M. M.Peiravi and J. Alinejad, "Hybrid conduction, convection and radiation heat transfer simulation in a channel with rectangular cylinder", *J. Thermal Analysis and Calorimetry*, Vol. 140, No. 1, pp 2733–2747 (2020).

[26] J. Alinejad and M.M.Peiravi, "Numerical analysis of secondary droplets characteristics due to drop impacting on 3D cylinders considering dynamic contact angle", *Meccanica*, Vol. 55, No. 1, pp. 1975–2002 (2020).

[27] M. M.Peiravi, J. Alinejad, D. Ganji and S. Maddah, "Numerical study of fins arrangement and Nano fluids effects on three-dimensional natural convection in the cubical enclosure", *J. Trans. Phenom. Nano Micro Scales*, Vol. 7, No. 2, pp 97-112 (2019).

[28] M. Ebrahimi and A. Keshavarz, "Sizing the prime mover of a residential micro-combined cooling heating and power (CCHP) system by multi-criteria sizing method for different climates", *J. Energy*, Vol. 54, No. 1, pp. 291-301, (2013)

[29] X. Q. Kong, R. Z. Wang and X. H. Huang, "Energy optimization model for a CCHP system with available gas turbines", *Appl. Therm. Eng.*, Vol. 25, No. 1, pp. 377–391, (2005).

[30] C. Yang, X. Wang, M. Huang, S. Ding and X. Ma, "Design and simulation of Gas Turbine-Based CCHP Combined with Solar and Compressed Air Energy Storage in a hotel Building", *J. Build. Eng.*, Vol. 153, No. 1, pp. 412-420, (2017)

[31] P. J. Mago, L. M. Chamra and J. Ramsay, "Micro-combined cooling, heating and power systems hybrid electric-thermal load following operation", *Appl. Therm. Eng.*, Vol. 30, No. 8, pp. 800-806, (2010).

[32] B. Rezaie and M. A. Rosen, "District heating and cooling: Review of technology and potential enhancements", *Appl. Energy*, Vol. 93, No. 1, pp. 2-10, (2012).

[33] R. Gomri, "Second law comparison of single effect and double effect vapour absorption refrigeration systems", *Energy Convers. Manage.*, Vol. 50, No. 5, pp. 1279–1287, (2009).

[34] J. H. Horlock, "Advanced Gas Turbine Cycles", An Imprint of Elsevier Science, Whittle Laboratory, Cambridge, UK, (2003).

How to cite this paper:

J. Pirkandi, A. Amiralaei and M. Ommian, "Performance analysis of a combined cooling, heating and power system based on micro gas turbine from the point of view of exergy,", *J. Comput. Appl. Res. Mech. Eng.*, Vol. 12, No. 1, pp. 77-93, (2022).

DOI: 10.22061/JCARME.2021.7514.1999

URL: https://jcarme.sru.ac.ir/?_action=showPDF&article=1643